Article

Improving Future Estimation of Cheliff-Mactaa-Tafna Streamflow via an Ensemble of Bias Correction Approaches

Mohammed Renima [1], Ayoub Zeroual [2,*], Yasmine Hamitouche [2], Ali Assani [3], Sara Zeroual [4], Ahmed Amin Soltani [5], Cedrick Mulowayi Mubulayi [2,6], Sabrina Taibi [7], Senna Bouabdelli [2], Sara Kabli [2], Allal Ghammit [2], Idris Bara [2], Abdennour Kastali [2] and Ramdane Alkama [8]

[1] Laboratory of Chemistry Vegetable-Water-Energy, Agronomy Department, University of Hassiba Benbouali, Chlef 02000, Algeria
[2] Water Engineering and Environment Laboratory, National Higher School for Hydraulics (ENSH-Blida), Blida 09000, Algeria
[3] Department of Environmental Sciences, University of Quebec at Trois-Rivières, 3351 Boulevard des Forges, Trois-Rivières, QC G9A 5H7, Canada
[4] LEGHYD Laboratory, Faculty of Civil Engineering, University of Sciences and Technology Houari Boumediene (USTHB), BP 32 El Alia Bab Ezzouar, Algiers 16111, Algeria
[5] VESDD Laboratory, Hydraulic Department, University of M'sila, M'sila 28000, Algeria
[6] Department of Natural Resources Management, Faculty of Agronomic Sciences, University of Kinshasa, Kinshasa P.O. Box 1031, Democratic Republic of the Congo
[7] LPPRE, Département des Sciences de l'Eau et l'Environnement, Université de Blida 1, Blida 09000, Algeria
[8] European Commission, JRC, Directorate D-Sustainable Resources, Bio-Economy Unit, TP124 Via E. Fermi, 2749, 21027 Ispra, Italy
* Correspondence: zeroualayoub34@yahoo.fr

Abstract: The role of climate change in future streamflow is still very uncertain, especially over semi-arid regions. However, part of this uncertainty can be offset by correcting systematic climate models' bias. This paper tries to assess how the choice of a bias correction method may impact future streamflow of the Cheliff-Mactaa-Tafna (CMT) rivers. First, three correction methods (quantile mapping (QM), quantile delta mapping (QDM), and scaled distribution mapping (SDM)) were applied to an ensemble of future precipitation and temperature coming from CORDEX-Africa, which uses two Representative Concentration Pathways: RCP4.5 and RCP8.5. Then, the Zygos model was used to convert the corrected time series into streamflow. Interestingly, the findings showed an agreement between the three methods that revealed a decline in future streamflow up to [−42 to −62%] in autumn, [+31% to −11%] in winter, [−23% to −39%] in spring, and [−23% to −41%] in summer. The rate of decrease was largest when using QM-corrected model outputs, followed by the raw model, the SDM-corrected model, and finally, the QDM-corrected model outputs. As expected, the RCP presents the largest decline especially by the end of the 21st Century.

1. Introduction

Global climate change and drought events are likely to have a significant impact on water resources worldwide [1]. Access to drinking water for the greatest amount of the population, as well as securing this often over-exploited and poorly managed resource, due to the impacts of global warming [2,3], have an impact on hydrological cycles at multiple scales [4,5]. Thus, watershed hydrological behavior modelling is essential for anyone concerned with natural hazards (floods, drought, groundwater salinization), as well as the prospect of global warming in this century and beyond [6–8].

Global climate model (GCM) outputs are widely used to study not only the global climate system response to both natural and anthropogenic radiative forcing, but also to assess the impact of climate change on environmental systems (e.g., hydrological systems).

However, global models with resolutions ranging from 100 to 200 km are unable to capture sufficient detail at the global regional scale. Therefore, bias adjustment techniques should be used to adjust the biased outputs of global and regional models because the use of regional climate models (RCMs) or statistical downscaling of global models can provide reliable climate information at the regional and local scales [9]. For instance, the precipitation and temperatures simulated by these climatic models in hydrological assessments can have significant systematic biases when compared to observed data [10,11]. Faulty conceptualization, spatial averaging across grid cells, and discretization can all be blamed for systematic errors in climate model outputs [12]. As a result, almost all studies assessing the impact of climate change require bias adjustment as a post-processing step.

Several bias adjustment algorithms for removing systematic errors from model outputs have recently been described in the literature. These algorithms establish a statistical relationship between a modelled and an observed climate variable on a regional scale or specific site over a calibration period (historical). Such relationships are then applied on a grid cell per point basis to correct some aspects of the biases in future climate simulations. The algorithms are designed to adjust one of the climate variables' statistical properties, such as the mean, variance, quantiles, number of rain days, and so on.

In comparison to alternative algorithms, several recent studies [12–14] emphasize the quantile mapping (QM) fitting algorithm as the most appropriate algorithm [15,16]. The QM algorithm, on the other hand, can artificially alter raw climate change signals, distorting future model simulation trends. According to [17], this alternative to signals of climate evolution is mainly due to the assignment of the same cumulative distribution function (CDF) used for observations of future simulations even though this distribution may change in future projections. Furthermore, the QM algorithm assumes that the modelled and observed distributions' biases remain constant over time [18,19]. Grenier [19] mentioned that this algorithm can assign to a particular variable an impossible value. These flaws in the QM algorithm necessitate techniques that effectively preserve changes in the simulated quantiles, address the problem of simulating impossible situations, and deal with the difficulty of removing temporal pattern bias (e.g., interannual variability). One adaptation of the standard QM method that preserves the raw signals of climate change is the detrended QM method. It is a non-parametric method using empirical quantiles [13,20,21].

Previous research has shown that while this method preserves the trend on a monthly scale, it alters the signals of raw climate change on a daily scale [22,23]. Quantile delta mapping (QDM) is a recently introduced adjustment to the QM algorithm developed by [24]. The QDM algorithm is based on the delta method and the detrended QM method [24]. This method, according to [25], preserves the trend for all quantiles while modifying the extreme indices. Switanek et al. [18] recently developed a new method that is structurally similar to QDM and considers the frequency of many days, climatic indices, and the probability of specific events. The three algorithms have been evaluated in several studies for correcting model-simulated bias of temperature and precipitation data.

Although several bias corrections have implications when corrected variables are used to assess impacts at the local scale, researchers have always focused their studies on comparing the corrected variables from simulations to the observed variables. In this context, numerous studies in the literature have attempted to improve the potential of RCM simulations in the analysis of the impact of climate change on water resources by developing or comparing bias correction algorithms that are applicable to the meteorological parameters required for the hydrological model [12,26–29]. Mpelasoka & Chiew. [26] demonstrated that the effect of three bias correction algorithms, namely the delta change method, daily scaling, and daily translation (DT), on computing the mean annual runoff is very small. Van Roosmalen et al. [27] discovered similar results when comparing four bias correction algorithms. Nguyen et al. [30] highlighted the relevance of the multivariate frequency bias correction approach compared to traditional correction approaches for hydrological modelling.

Based on the above insights, the main objective of this paper is to study how these three bias correction algorithms modulate the climate change signal of precipitation and temperature over six mountainous watersheds of northwestern Algeria and the resulting impact on their runoff using a lumped conceptual Zygos hydrological model.

Although a number of studies have been conducted in Algeria to investigate the harmful effects of climate change on the availability of water resources and the identification of regional and local drought episodes [31,32], only a small number of studies have been conducted to investigate the future availability of water resources, particularly in northwestern Algeria regions, which already are experiencing water scarcity [31]. Existing studies have shown a drastic decrease in rainfall of about 30% in western Algeria, which caused serious hydrological crises and significantly affected the plains of this region known for its fertility [31–33]. Water stress has been experienced over the past few decades. In the Tafna and Macta basins in the country's extreme west, [33] discovered a significant dry trend in base flows between 1972 and 1992 on annual and seasonal scales of 50% to 71%. This reduction was marked on the basins located in plains as on the basins in relief (Beni-Bahdel, Pierre de chat, Chouly and Khemis), although they are the least disturbed by human activities given their strong gradient of altitude [34]. The western region of northern Algeria has been identified as a region prone to increasing temperatures and aridity in the future as a result of decreased precipitation and increased temperature.

2. Study Area

The research was based on three basins in Algeria's far northwest, which are located in the southern Mediterranean area, namely the Cheliff, Macta, and Tafna basins (Figure 1), in which the Cheliff basin occupies an area of 44,630 km^2 and is located between the geographic coordinates 34° to 36°30′ north latitude and 0° to 3°30′ east longitude, exhibiting the shape of an axe-blade running north–south. It has an arid to semi-arid Mediterranean climate in the south, with warm Saharan influences in the north and east, and a mild climate in the north and east. Precipitation is very regular in time and space, with two extreme zones: one is wet with an annual average of 524 mm to 658 mm, and the other is less rainy with an annual average of 350 mm. The Cheliff watershed is located in the semi-arid to moderately temperate climate zone, with an average inter-annual precipitation of 571 mm and average monthly temperatures ranging from 10° in January to 28° in July and August, with an average yearly temperature of 18 °C.

The Cheliff furrow is compartmentalized into three basins (higher, middle, and lower Cheliff) separated by tow thresholds such as bedrock, the threshold of Ain Defla and, therefore, the threshold of Oum D'rou further west. Many permeable geological formations contain groundwater; the oldest are assigned to the Jurassic period, and therefore, the most up-to-date correspond to the quaternary alluvium. Within the northern part of the study area, the two Tellian chains are poor resources, and it is difficult to take advantage of them directly; the permeable levels (limestone and sandstone) are generally less developed and encased in powerful formations that have a very low permeability.

2.1. The Basin of Macta

The basin of Macta occupies a complete area of 14,410 km^2; its geographical position is between −1.25° west and 0.60° east in longitude and between 34° and 36° north in latitude. It is limited within the northwest by the mountain ranges of Tessala, within the south by the highlands of Maalif, within the west by the plateaus of Telagh, and within the east by the Saida Mountains [35]. The Macta basin is bordered in the north by the Mediterranean Sea, to the south by the mountains of Saida (1201 m) and the Daya Mountains (1356 m), and to the southwest by the mountains of Tlemcen, including the mountains of Beni Chougrane and, therefore, the plain of Mohamadia [35]. The typical annual rainfall ranges from 206 mm in the southern part to 380 mm in the Saïda Mountains. The mean monthly temperature ranges from 11° in January to 26 °C in July and August. The Macta watershed is drained by

two major rivers, namely: El-Hammam Wadi in the east and Wadi Mekkera (called Wadi Mebtouh downstream) in the west [35].
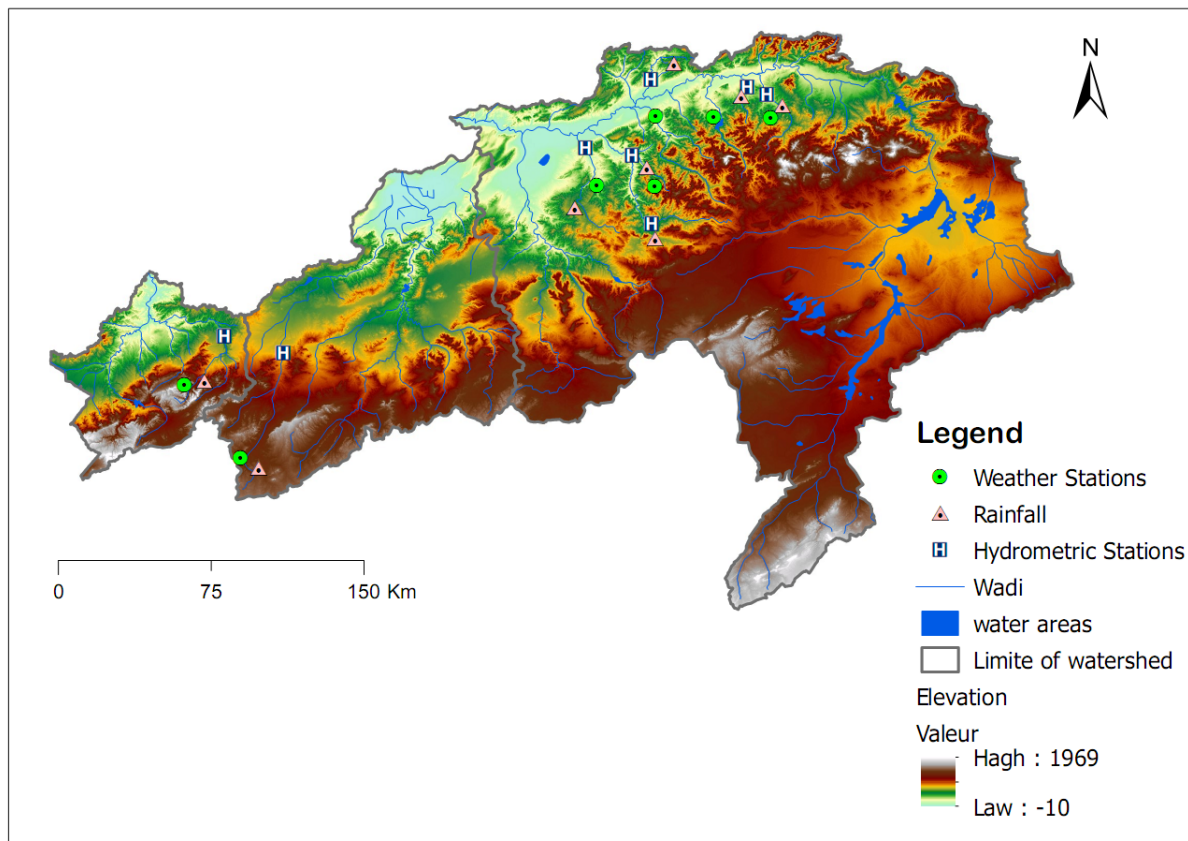

Figure 1. Cheliff-Mactaa-Tafna basin climate and streamflow stations.

2.2. The Basin of Tafna

The Tafna's catchment basin is located in Algeria's extreme northwest. One of the most important wadis in the west crosses it. Tafna, with over 6900 km^2, flows from west to east, from Morocco to the Mediterranean (near Beni Saf), and the length of the greatest river bed is 759 km (Figure 1). The basin is dominated to the south by a WSE–ENE-oriented mountainous bar (800–1400 m), while the plain areas of Maghnia, Hannaya, and Sidi Abdelli dominate to the north. This orographic structure, which is dominated in the north by the small-scale Traras mountains (1081 m a.s.l.), creates an effective precipitation barrier, explaining the aridity of the Maghnia plain [36]. The Tafna basin's climate is equivalent to that of the Northern Africa Mediterranean region, which is warm and humid, with the two hottest months being July and August, with an average temperature of 26 °C [33]. The Tafna River's hydrographic network consists mostly of two arteries: Wadi Tafna in the west and Wadi Isser in the east, and it originates in the Tlemcen Mountains.

3. Dataset Used

Various climate data were used for climate change impact assessment studies using a hydrological model at the monthly scale, including streamflow, precipitation, temperature, and evaporation.

3.1. Hydrological Model Data

The Zygos model requires the monthly time series of precipitation, potential evapotranspiration, runoff, as well as groundwater extraction (if these data are available) to simulate the watershed response. The Algerian National Hydraulic Resources Agency provided climate data for seven stations located within and near the Cheliff-Mactaa-Tafna

(CMT) basins from 1975 to 2012 (Table 1 and Figure 1). Nevertheless, the gaps in the overall precipitation and temperature time series do not exceed 8%. To detect outliers and fill gaps in the data series, three steps were used: visual inspection, comparison with the nearest station in the same area, and regression relationships between neighboring stations.

Table 1. Rainfall stations from the National Agency ANRH.

Stations Code	Name Stations	Watershed	Latitude	Longitude	Measurement Period
PV011901	El Touaibia	Cheliff	1°94′	36°12′	1990–2012
PV012004	Tikezal	Cheliff	1°75′	36°19′	1989–2012
PV012201	Larabaa Ouled Fares	Cheliff	1°24′	36°24′	1971–2012
PV012507	Oued Lili	Cheliff	1°26′	35°52′	1975–2005
PV012703	Kenanda Ferme	Cheliff	0°82′	35°65′	1978–2005
PV110102	Ras Elma	Mactaa	−0°83′	34°46′	1980–2010
PV160601	Chouly	Tafna	−1°13′	34°86′	1975–2012

3.2. Streamflow/River Discharge Data

The Algerian National Hydraulic Resources Agency manages several gauging stations in the CMT basin, which are in small tributaries of the CMT River and cover small watersheds. All but eight of these stations (Table 2 and Figure 1) are outside the scope of this research analysis due to significant data gaps, and that the majority of stations have not been operational for an extended period.

Table 2. Characteristics of hydrometric stations.

Station Code	Name Stations	Watershed	Wadi	Latitude	Longitude	Surface (km^2)	Measurement Period
Qm011905	Bir Ouled Tahar	Cheliff	Zeddine	36°19′	1°85′	450	1990–2008
Qm012004	Tikezal	Cheliff	Tikezal	36°19′	1°75′	130	1990–2012
Qm012201	Larabaa Ouled Fares	Cheliff	Ouahrane	36°22′	1°21′	262	1983–2011
Qm012501	Oued Lilli	Cheliff	Tiguiguest	35°59′	1°24′	1612	1975–2006
Qm012601	Ammi Moussa	Cheliff	Rhiou	35°86′	1°12′	1937	1975–2006
Qm012701	Djidiouia	Cheliff	Djidiouia	35°92′	0°88′	836	1975–2006
Qm110101	Haciabia	Mactaa	Mekerra	34°69′	−0°75′	941	1980–2001
Qm160601	Chouly	Tafna	Chouly	34°86′	−1°13′	167	1975–2006

3.3. Climate Scenario Data and Bias Correction Method

To assess the impact of climate change on the Cheliff-Mactaa-Tafna (CMT) basins' hydrology, the monthly precipitations and monthly temperature data simulated from the Rossby Centre Regional Climate Model (RCA4) driven by the MPI-ESM-LR General circulation model from the Coupled Model Intercomparison Project—Phase 5 (IPCC5) [37], available within the CORDEX project, were extracted for each climate station during the 1971–2100 period. The entire dataset simulated spans 1971–2100, consisting of a historical period (1971–2005) and two projection periods (2025–2050 and 2075–2100). The projection period was forced by two Representative Concentration Pathway (RCP) scenarios, RCP4.5 and RCP8.5. The data extracted from the RCA4-MPI-ESM-LR climate model (monthly precipitations, monthly temperature) deviate from the data observed at the climate stations. Therefore, bias adjustment is a required post-processing step in almost all studies assessing the impact of climate change. We adjusted the data bias generated from the RCA4-MPI-ESM-LR regional climate model using three methods: quantile mapping, scaled distribution mapping, and quantile delta mapping before predicting the possible change in the future hydrology of the Cheliff-Mactaa-Tafna (CMT) basins. Afterwards, the same procedure that was used in the historical period for validation was applied for the two future periods for discharge simulation. The three bias correction algorithms are summarized in the Supplementary Material S3 to avoid filling up the text with formulas.

3.4. Hydrological Modeling Using Zygos

The Zygos model is a conceptual rainfall–runoff modeling tool that employs a series of reservoirs (Figure 2) to represent the soil and subsoil schematically. The total flow is composed by four principal components [38] including the direct discharge, QDt, caused by the presence of impervious formations, through which the proportion of rainfall is transformed directly into runoff; the surface discharge, QQt, which results from an immediate reaction due to soil saturation; the subsurface discharge, QIt, which is a slow response caused by the lateral (horizontal) movement of water, infiltrating into the soil; and the base discharge, Qbt, being the lower soil layers' (aquifer) response, by means of employing springs. Simulating subwatershed flow is a similar approach to Thornthwaite's model [38] (National Technical University of Athens (NTUA) Research Team, 2010). It is a lumped conceptual water balance model that runs on a monthly time step in most cases. On the one hand, the model's input data are monthly time series of precipitation Pt, potential evapotranspiration Ept, runoff Qt, and the extraction rate from groundwater PUMPt; on the other hand, the model's outputs are runoff at the watershed outlet Qt (surface water and groundwater), actual evapotranspiration Et, and the watershed outlets. A detailed description of this model is presented in Charizopoulos and Psilovikos. [39], among others.
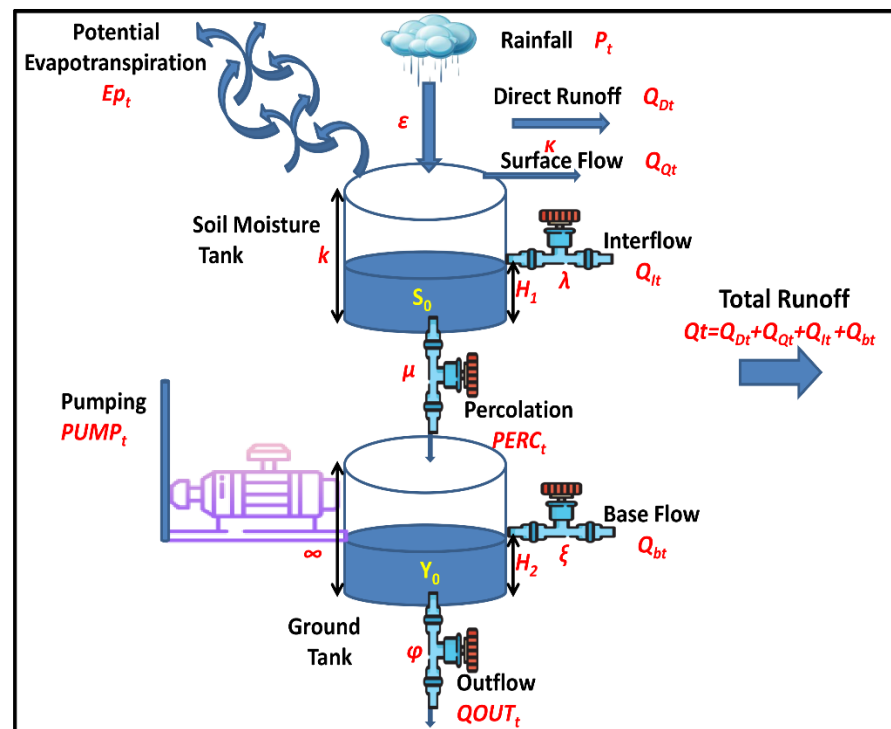

Figure 2. Schematic representation of the hydrologic processes of the conceptual hydrological model Zygos (Adapted from Kozanis et al. [38]).

3.5. Parameter's Description

The Zygos model includes eleven parameters (Table 3) that define the flow distribution or reservoir characteristics (initial level and capacity, H_1 or H_2 values) [39]. This may result in the possibility of over-parameterization of the same hydrosystem using Zygos, as well as the ability of compensation between the different models' parameters used to model the output data. Several parameters can take values corresponding to the limit values allowed in calibration [39]. The model's state variables are soil moisture and groundwater storage, which require information about the initial conditions S0, K, and Yo, respectively. To avoid weighing down the text with formulas, the descriptions of the model parameters are summarized in Table 3 [39]. The detailed mathematical description of the model operation is presented in Charizopoulos and Psilovikos [39] and Charizopoulos et al. [40].

Table 3. Parameters of the manual calibration of the rainfall–runoff model Zygos (Reprinted from Kozanis et al. 2010 [38] and Charizopoulos and Psilovikos [39]).

Parameters	Description
ε	Rainfall proportion available for the achievement of direct evapotranspiration.
κ	The rainfall excess proportion, appearing as direct runoff, caused by the occurrence of impermeable formations. Through them, the rainfall proportion is transformed directly into runoff. Essentially, it is the percentage of impermeable surface and expresses the percentage that runs off directly without percolating the soil.
k	The capacity of the soil moisture tank, which expresses the maximum storage capacity of the ground (mm).
So	Initial reserve of the soil moisture.
λ	Discharge rate of the soil moisture tank, for the creation of subsurface flow.
H_1	Reserve threshold of the soil moisture tank, for the creation of subsurface flow.
μ	Discharge rate of the soil moisture tank, for the creation of infiltration.
ξ	Discharge rate of the groundwater tank, for the creation of base flow.
H_2	Reserve threshold of the groundwater tank, for the creation of base flow.
φ	Discharge rate of the groundwater tank, for the creation of subsurface outflow.
Υο	Initial reserve of the groundwater tank.

3.6. Performance Criteria

Each reservoir represents an essential physical process carried out during the water flow within the watershed. The Nash coefficient [41] was selected as the criterion for evaluating the error between simulated and observed runoff. It is a transformed and normalized measure of the RMSE overall (normalized to the variance of the observed hydrograph) [41]. The Nash–Sutcliffe coefficient (NSE) is considered a typical indicator of a good fit for hydrologic models, given by Equation (1).

$$NSE = 1 - \frac{\sum_{i=1}^{N}(Qo - Q_E)^2}{\sum_{i=1}^{N}(Qo - Qoave)^2} \tag{1}$$

where: Q_o = the observed runoff, Q_E = the runoff estimated by the model, Q_{oave} = the mean value of observed runoffs, N = the total number of observations. The coefficient value ranges from $-\infty$ to 1. If R < 0, the fit of the model is considered poor, whereas when the value is near 1, the simulated time series provides a better fit compared to the mean observed value Q_{oave}.

4. Results

The Zygos model must be tested before being used for research or operational reasons. This procedure is known as model calibration/validation, and it was used for each basin in the study area. The Zygos model was automatically calibrated and validated using the reference periods' monthly precipitation, evaporation, and discharge data; the results are given in Table 4.

Validation was performed for the stations of Bir Ouled Tahar, Ammi Moussa, and Chouly from 2003 to 2008, 1998 to 2004, and 1997 to 2004, respectively. For the two phases "calibration/validation", the Pearson correlation coefficient ranged between 0.66 and 0.95.

The average size of these basins explains the model's good fit to the observed data. In terms of the general dynamics of river flows at the stations of Larabaa Ouled Fares, Oued Lilli, and Djediouia, we found that this dynamic is well reproduced because the validation yielded Pearson correlation coefficients ranging from 0.45 to 0.68, reflecting the model's average quality in reproducing the hydrological reality that characterizes these basins. Furthermore, the short water path results in a quick concentration time. This reduces losses due to seepage, evaporation, and absorption.

Table 4. Simulation parameters.

	Stations	Ammi Moussa	Chouly	Djediouia	Haciaba	L. Ouled Fares	Oued Lilli	Tikezal	Bir Ouled Tahar
Calibration	Period	1980–1997	1979–1996	1979–1996	1980–1995	1983–2000	1979–1996	1990–2004	1990–2002
	NSE (calibration)	0.56	0.98	−0.84	0.16	−5.81	0.55	0.62	0.60
	RMSE	40.67	3.61	9.29	5.53	60.92	4.67	4.29	24.91
Zygos modelparameters	κ	0.247	0.04	0.154	0.013	0.694	0.131	0.01	0.023
	μ	0.023	0.99	0.22	0.839	0.4	0.188	0.886	0.017
	ε	0.547	0.99	0.99	0.099	0.01	0.399	0.813	0.189
	H_1	39.42	133.99	13.52	101.23	3.80	40.09	6.00	0.74
	H_2	68.99	96.88	263.29	158.71	5.00	115.60	72.23	60.40
	λ	0.104	0.889	0.145	0.378	0.99	0.318	0.99	0.029
	ξ	0.341	0.225	0.77	0.659	0.699	0.89	0.99	0.63
	φ	0.01	0.03	0.35	0.23	0.01	0.03	0.02	0.15
	k	120.28	156.9	111.85	182.73	170.14	100.01	195.61	111.28
	So	14.62	17.68	11.11	16.6	20.26	10.37	9.61	8.39
	Υo	5.09	5.00	226.84	271.23	295.31	20.03	290.00	116.20
	Objective function	0.594	0.767	0.41	0.071	0.0736	0.696	0.018	0.171
Validation	Period	1998–2004	1997–2004	1997–2004	1996–2001	2001–2007	1997–2004	2005–2011	2003–2008
	NSE (validation)	1.00	0.96	−1.48	0.85	−0.45	0.02	0.37	0.29
	RMSE	0.84	2.56	10.65	0.82	27.19	3.42	23.34	42.36

4.1. Parameter of Simulation

The results of rainfall–runoff modeling can be more dependent on the quality of the input data than on the model [42]. The optimal value of the Nash coefficient (Equation (1)) or the objective function that expresses the differences between simulated and observed values was varied between −2.74 and 0.77, and it was reached with the combination of the parameters presented in Table 4. This value is high, indicating that the simulated runoff adapted well to the measured runoff. Because of variations in altitude and average yearly temperatures, the proportion of rain available for direct evapotranspiration, indicated by the parameter ε, varied (from 0.01 to 0.99) from one basin to another. Due to the location of the area study in the most extensive karst system in northern Algeria and which presents the widest natural groundwater reservoir in the west (S0: 8.39 to 20.26 mm), the karst aquifers of this region are considered as the largest natural reservoirs of rainfall in north Algeria. The direct runoff, maximum storage capacity, subsurface flow (groundwater), and discharge rate from the soil moisture reservoir for the development of infiltration, as expressed by the parameters κ, k, λ, H_1, and μ, suggest that runoff is superior to infiltration. This is related to the occurrence of semi-permeable formations in the area. In addition, the parameter ξ varies from 0.225 to 0.99 and H_2 from 5 to 263.29 mm, which are crucial in generating the base flow. The outflow coefficient φ (0.01 to 0.35) is related to the karstic mass of Chlef-Relizane, Saida, and Telemcen, which flows towards the plains of Cheliff, Ghriss-Mascara, and Maghnia.

4.2. Changes in Evapotranspiration

The projected temperature increase in the Cheliff, Mactaa, and Tafna catchments would result in an increase in ETP from 33% to 41% and from 29% to 38% by 2050 for the RCP4.5 and RCP8.5 scenarios, respectively, and from 47% to 57% and 77% to 94% by 2100 for the two scenarios RCP4.5 and RCP8.5 (Table S1 and Figure 3). The largest rise is reported by the stations of Ammi Moussa, Oued Lilli, and Haciaba, with 41% by 2050 and 94% by 2100. In general, the average rate of rise for the 2050 and 2100 timeframes ranges from 34% to 37% and from 53% to 85%, respectively.

4.3. Projected Precipitation

Future precipitation data for Bir Ouled Tahar, Tikezal, Larabaa Ouled Fares, Ammi Moussa, Oued Lilli, Kenanda Farme, Ras Elma, and Chouly in the CMT basins were

corrected using three bias correction techniques: the QM, SDM, and QDM algorithms. In our study, the RCP4.5 and RCP8.5 climate scenarios were evaluated for two future periods, 2050 and 2100, compared to the reference period (1975–2012). After adjusting the biases of the raw precipitation sample, the study found that average annual precipitation in the CMT basins would generally decline in the future (Table 5 and Figure S1).
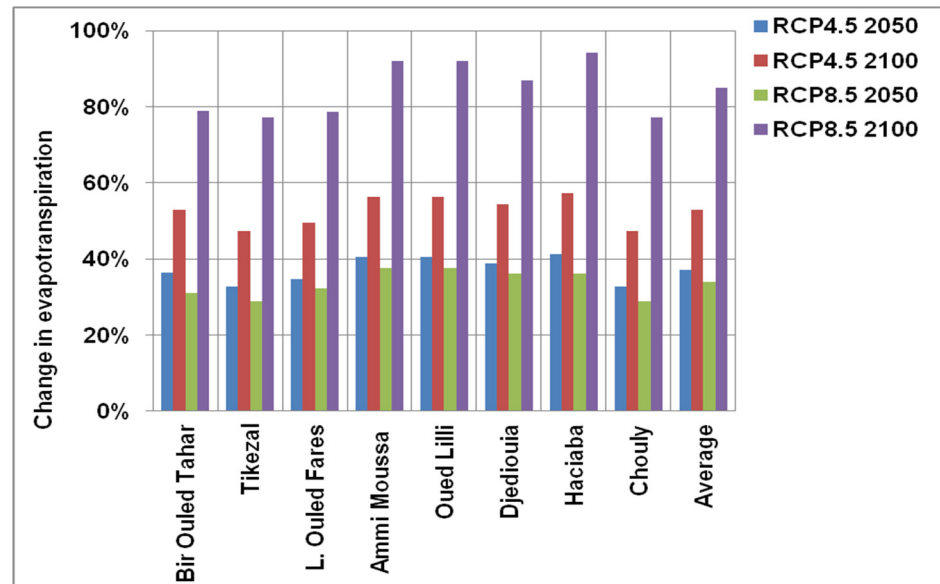

Figure 3. Changes in evapotranspiration under two scenarios (RCP4.5 and RCP8.5).

Table 5. Annual precipitation mean changes in the CMT basins from the baseline period (1975–2012).

STATIONS	Quantile Mapping (QM)				Scaled Distribution Mapping (SDM)			
	RCP4.5 2050	RCP4.5 2100	RCP8.5 2050	RCP8.5 2100	RCP4.5 2050	RCP4.5 2100	RCP8.5 2050	RCP8.5 2100
Bir Ouled Tahar	−27%	−30%	−31%	−51%	−22%	−25%	−16%	−38%
Tikezal	−57%	−55%	−44%	−53%	−42%	−38%	−25%	−37%
Larabaa Ouled Fares	−16%	−15%	−15%	−40%	−17%	−14%	−14%	−30%
Ammi Moussa	−20%	−30%	−25%	−48%	−5%	−17%	−16%	−27%
Oued Lilli	−16%	−27%	−27%	−49%	−3%	−6%	−15%	−27%
Djediouia	−22%	−28%	−27%	−37%	−17%	−30%	−12%	−20%
Haciaba	−42%	−41%	−46%	−54%	−23%	−30%	−33%	−41%
Chouly	−18%	−30%	−29%	−47%	0%	−6%	−11%	−24%

STATIONS	Quantile Delta Mapping (QDM)				Model (RAW)			
	RCP4.5 2050	RCP4.5 2100	RCP8.5 2050	RCP8.5 2100	RCP4.5 2050	RCP4.5 2100	RCP8.5 2050	RCP8.5 2100
Bir Ouled Tahar	−9%	−12%	−15%	−38%	−24%	−26%	−24%	−46%
Tikezal	−43%	−39%	−27%	−38%	−50%	−48%	−35%	−47%
Larabaa Ouled Fares	−11%	−11%	−11%	−38%	−21%	−28%	−27%	−47%
Ammi Moussa	−12%	−21%	−16%	−37%	−9%	−19%	−20%	−40%
Oued Lilli	−4%	−16%	−16%	−37%	−9%	−19%	−20%	−40%
Djediouia	−16%	−9%	−22%	−32%	−13%	−23%	−25%	−40%
Haciaba	51%	67%	64%	66%	−15%	−16%	−20%	−27%
Chouly	71%	56%	58%	35%	−21%	−23%	−21%	−41%

For the QM-RCP4.5 climate scenario, the change in mean annual precipitation ranges from −15 to −57%, while for the QM-RCP8.5 high-level climate scenario, the change is from −15 to −54%. For the RCP4.5 climate scenario, decreases range from −3% to 42%, whereas for the RCP8.5 climate scenario, decreases range from −11% to −41%. For the

RCP4.5 climate scenario, the correction via the QDM approach revealed decreases ranging from −4% to −43% and increases up to +71%. The RCP8.5 climatic scenario showed similar results, with decreases ranging from −11% to −38% and increases of up to +66%. Finally, over all future periods, the decreases in raw climate model outputs range from −9% to −50% for the RCP4.5 climate scenario and from −20% to −47% for the RCP8.5 climate scenario (Table 5 and Figure S1).

4.4. Streamflow Projected

The Zygos hydrological model calibrated and validated at the monthly scale for the reference period (1975–2012) was used to simulate future flows in the CMT basin for two future periods under two scenarios. The outputs of the Zygos model were compared to those of the reference period for the two projected periods 2050 (2025–2050) and 2100 (2075–2100) under the two climatic scenarios. The two climate scenarios resulted in moderate reductions in the average annual deficit for all future periods, due to the anticipated decrease in precipitation. However, the RCP4.5 and RCP8.5 climate scenarios for the year 2100 showed a decrease in the deficit for all methods due to a projected increase in temperature, which causes an increase in evaporation rather than a decrease in precipitation, except for the QDM method, which showed an increase in the deficit (Table 6; Figure S2). We detected a trend of decreasing average monthly flows in the RCP4.5 scenario and a mixed pattern in the RCP8.5 scenario for the two periods analyzed and all stations studied. The change rate in annual mean flows spans from −91% to −3% for the QM-RCP4.5 climate scenario and from −92% to −6% for the QM-RCP8.5 climate scenario.

Table 6. Annual streamflow mean changes in the CMT basins from the baseline period (1975–2012).

STATIONS	Quantile Mapping (QM)				Scaled Distribution Mapping (SDM)			
	RCP4.5 2050	RCP4.5 2100	RCP8.5 2050	RCP8.5 2100	RCP4.5 2050	RCP4.5 2100	RCP8.5 2050	RCP8.5 2100
Bir Ouled Tahar	−10%	−3%	−27%	−51%	−18%	−19%	−6%	−44%
Tikezal	−90%	−91%	−36%	−32%	−38%	−52%	27%	42%
Larabaa Ouled Fares	−7%	−4%	−6%	−28%	−10%	−7%	−3%	−21%
Ammi Moussa	−22%	−23%	−9%	−50%	−16%	−15%	−6%	−31%
Oued Lilli	−27%	−23%	−24%	−48%	−9%	−18%	−8%	−29%
Djediouia	−18%	−19%	−7%	−11%	−18%	−24%	−2%	−7%
Haciaba	−75%	−75%	−77%	−80%	−69%	−71%	−73%	−75%
Chouly	−61%	−58%	−60%	−92%	−55%	−35%	−58%	−93%

STATIONS	Quantile Delta Mapping (QDM)				Model (RAW)			
	RCP4.5 2050	RCP4.5 2100	RCP8.5 2050	RCP8.5 2100	RCP4.5 2050	RCP4.5 2100	RCP8.5 2050	RCP8.5 2100
Bir Ouled Tahar	21%	24%	26%	−35%	−1%	−1%	−5%	−53%
Tikezal	−36%	−77%	46%	22%	−88%	−91%	−22%	−41%
Larabaa Ouled Fares	−1%	0%	−2%	−25%	−13%	−18%	−44%	−37%
Ammi Moussa	−14%	−17%	5%	−39%	−5%	−5%	−6%	−47%
Oued Lilli	−20%	−19%	−11%	−36%	−23%	−19%	−31%	−50%
Djediouia	−4%	−72%	5%	6%	−10%	−22%	−27%	−58%
Haciaba	−43%	−37%	−38%	−38%	−66%	−66%	−68%	−70%
Chouly	118%	63%	−70%	−55%	−70%	−45%	−52%	−92%

The decreases for the SDM technique range from −71% to −7% for the RCP4.5 climate scenario and from −93% to −2% for the RCP8.5 climate scenario. For this last scenario, an increase in flow of around +42% is expected in the Tikezal station. In addition, for the RCP4.5 climatic scenario, the QDM approach revealed drops in annual mean flows ranging from −77% to −1% and rises to +118%. The same results were reported for the RCP8.5 climatic scenario, with losses ranging from −2 to −70% and gains reaching +46%. Finally,

for the raw climate model output, flow decreases range from −1% to −91% for the RCP4.5 climate scenario and from −92% to −5% for the RCP8.5 climate scenarios for all future periods (Table 6 and Figure S2).

4.5. Projected Season Precipitation

To evaluate the impact of climate change seasonal runoff, we established the seasons of autumn from September to November, winter from December to February, spring from March to May, and summer from June to August in this study. Under both scenarios (RCP4.5 and RCP8.5), the outputs from the three corrected techniques QM, SDM, and QDM, as well as the uncorrected version of the models (raw) showed that precipitation in the study region will continue to decline during the period 2075–2100. The decrease in precipitation will be more important in the RCP8.5 scenario than under the RCP4.5 scenario (Figures 4–7 and Tables S2–S5). According to the RCP 4.5 scenario (Figures 4–7 and Tables S2–S5), the MPI model predicted a decrease in precipitation between −17 and −58% in autumn, −3 and −56% in winter, and −25 and −74% in spring by the end of the 21st Century, compared to the QM method.
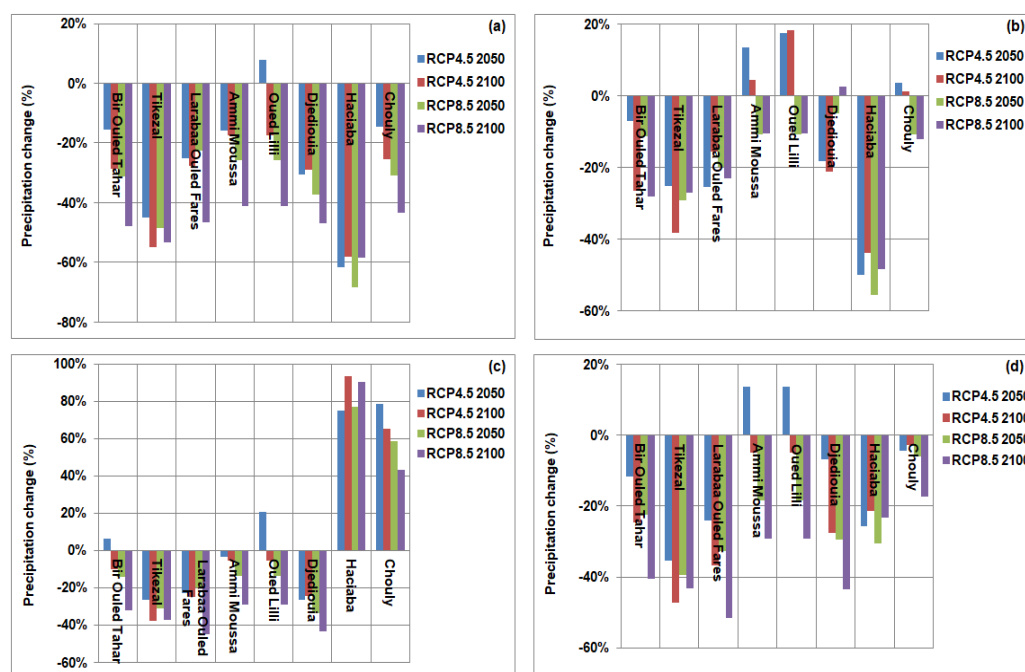
Figure 4. Changes in autumn precipitation relative to the historical period under two scenarios (RCP4.5 and RCP8.5): (**a**) quantile mapping, (**b**) scaled distribution mapping, (**c**) quantile delta mapping, and (**d**) model (RAW).

The SDM approach showed a decrease in precipitation ranging from 1% to −44% in autumn, from −18% to −43% in winter, and from −14% to −58% in spring. The QDM approach, on the other hand, showed a smaller rate of change (increase and decrease) of precipitation than the other methods, with this rate varying between −38% and 93% in autumn, −43% and 17% in winter, and −41% and 89% in spring. The pessimistic scenario RCP 8.5 reduced the precipitation more than the pessimistic scenario RCP4.5. The MPI model likewise showed larger precipitation reductions for the period 2075–2100, ranging from −41 to −59% in autumn, from −17 to −70% in winter, and from −54 to −94% in spring for the QM technique. The SDM approach (Figures 4–7 and Tables S2–S5) revealed a rate of change in precipitation ranging from 3% to −48% in autumn, from −24% to −48% in winter, and from −37% to −80% in spring. The QDM approach, on the other hand, showed the smallest decrease in precipitation when compared to the other two methods. This rate of decrease/increase fluctuated between −45% and 91% in autumn, −33% and

98% in winter, and −61%t and 17% in spring. It should also be noticed that the simulated precipitation after bias correction is much higher than the raw data for the prediction periods 2025–2050 and 2075–2100. This is due to the model data being corrected in relation to the observed precipitation, which was significantly underestimated by the MPI model during the historical period.
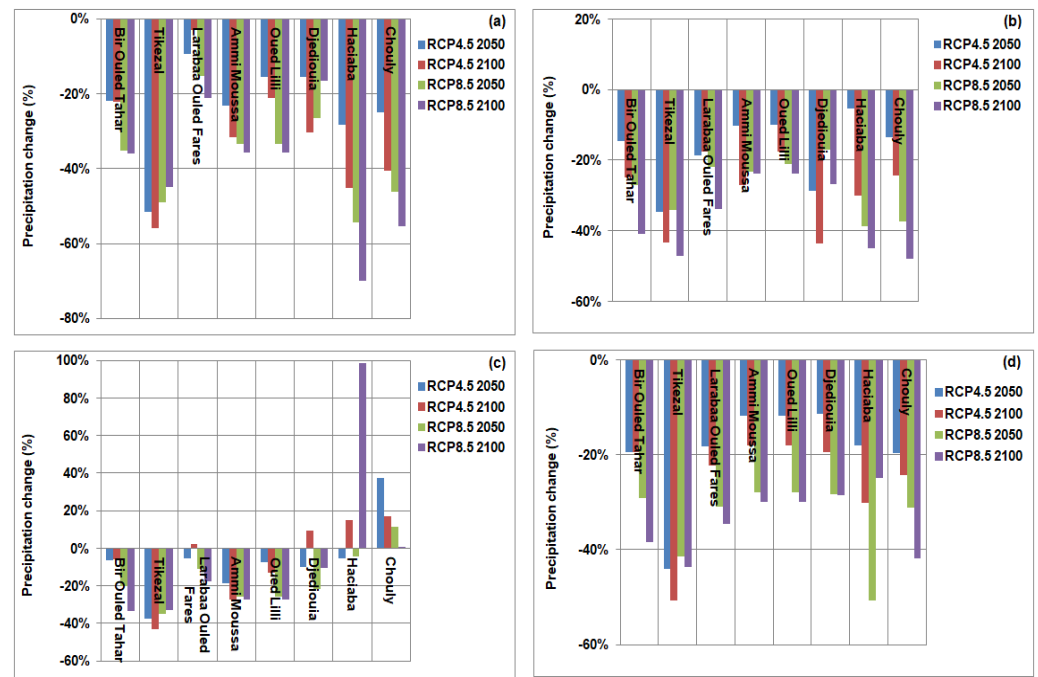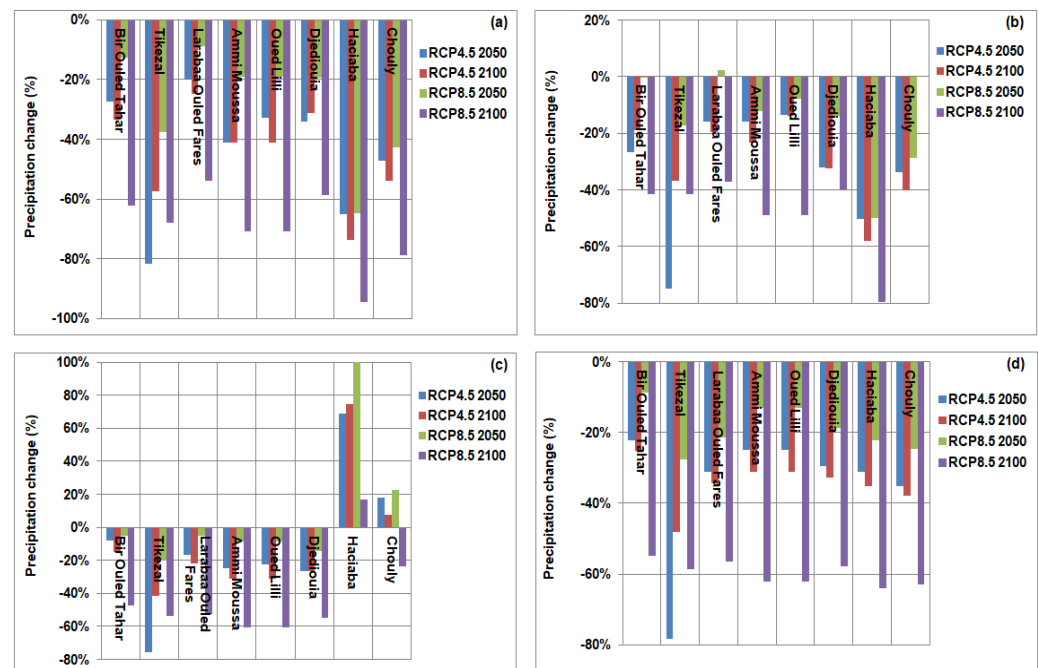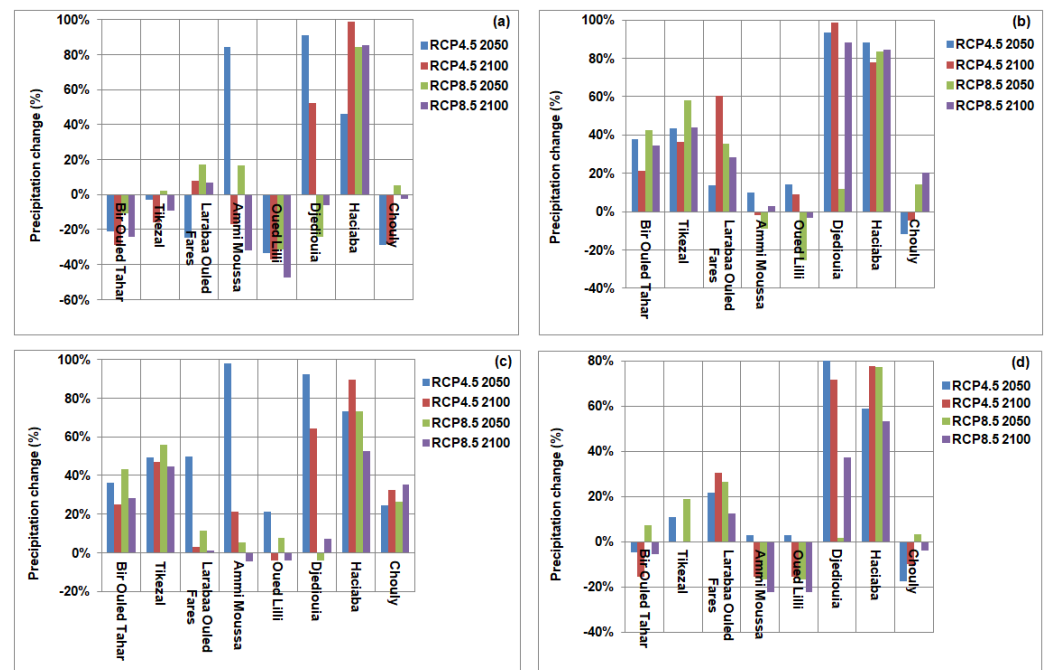

Figure 5. Changes in winter precipitation relative to the historical period under two scenarios (RCP4.5 and RCP8.5): (**a**) quantile mapping, (**b**) scaled distribution mapping, (**c**) quantile delta mapping, and (**d**) model (RAW).

Figure 6. Changes in spring precipitation relative to the historical period under two scenarios (RCP4.5 and RCP8.5): (**a**) quantile mapping, (**b**) scaled distribution mapping, (**c**) quantile delta mapping, and (**d**) RAW.
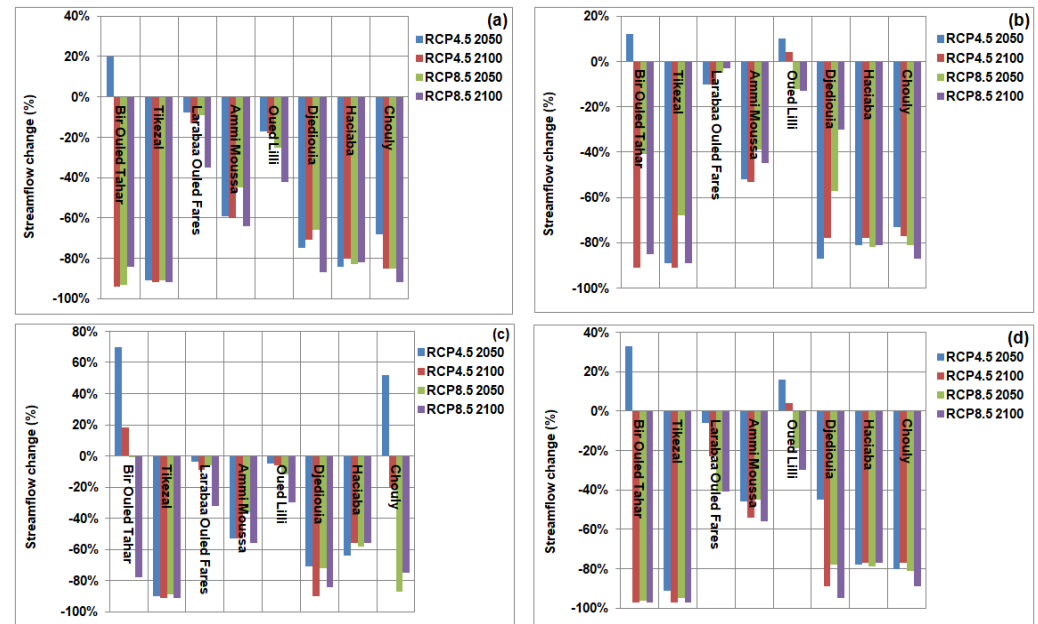
Figure 7. Changes in summer precipitation relative to the historical period under two scenarios (RCP4.5 and RCP8.5): (**a**) quantile mapping, (**b**) scaled distribution mapping, (**c**) quantile delta mapping, and (**d**) RAW.

4.6. Seasonal Streamflow Projections

Tables S6–S9 show the percentage change rates of seasonal flow in the CMT basin simulated by the Zygos hydrological models based on the outputs corrected by the three methods QM, SDM, and QDM and the raw model data MPI-ESM-LR model under the RCP4.5 and RCP8.5 scenarios for the two future periods 2025–2050 and 2075–2100. The results of the simulations of the three methods QM, SDM, and QDM, as well as the raw model output showed that the seasonal flow has a tendency to decrease during the period 2075–2100 under the two scenarios and during all seasons except summer under the RCP4.5 and RCP8.5 scenarios.

Under the RCP4.5 climate scenario, the rate of change of autumn flows (Table S6 and Figure 8) varies from +20% to −91% in the short term (2050s) and from −13% to −92% in the long term (2100s). The rate of change under the RCP8.5 scenario, on the other hand, ranges from −9% to −91% by 2050 and from −35% to −92% over the 2100 horizon. Under the RCP4.5 scenario, the adjustment using the same algorithm (QM) revealed a rate of change in winter (Figure 9)ranging from −89% to 60% and from −90% to +29% by 2100. With the RCP8.5 climate scenario, this rate of change is somewhat positive, ranging from −72% to +71% and −84% to 79% by 2100. The rate of change for future spring flows (Table S8 and Figure 10) varies between −94% and 63 percent for the two climatic scenarios. Using the QM-algorithm-corrected models, an increase in summer flows (Table S9 and Figure 11) was found at three stations. This increase varied between +12% and +168% for the two time periods (2050 and 2100) and two scenarios. Summer flow is expected to decrease in the other stations (reaching −100 percent).

Under the RCP4.5 climate scenario, the rate of change of the predicted autumn flows varies between −89% and +12% in the near term (2050s) and +4% to −91% in the long term (2100s) when utilizing precipitation data corrected by the SDM approach (Table S6 and Figure 8). The rate of change in the RCP8.5 scenario, on the other hand, ranges from −82% to −5% and from −3% to −89% by 2100. The correction using the same algorithm (SDM) (Table S7 and Figure 9) reveals a rate of change in winter ranging from −47% to +46% and from −63% to +30% by 2100 under the RCP4.5 scenario. With the RCP8.5 climate scenario, this rate of change is somewhat positive, ranging from −42% to +105%

and −88% to +48% by 2100. Using the SDM-algorithm-corrected models, an increase in future summer flows was observed at two stations (Ammi Moussa and Oued Lilli station) (Table S9 and Figure 11). The rate of change for future spring flows (Table S8 and Figure 10) varies between −98 percent and +91 percent for the two climate scenarios. This rise ranges between +12% and +181% for the two time periods (2050 and 2100) and two scenarios. Summer flow is expected to fall at the other stations (varying between −6 and −99%).

Figure 8. Changes in autumn streamflow relative to the historical period under two scenarios (RCP4.5 and RCP8.5): (**a**) quantile mapping, (**b**) scaled distribution mapping, (**c**) quantile delta mapping, and (**d**) model RAW.
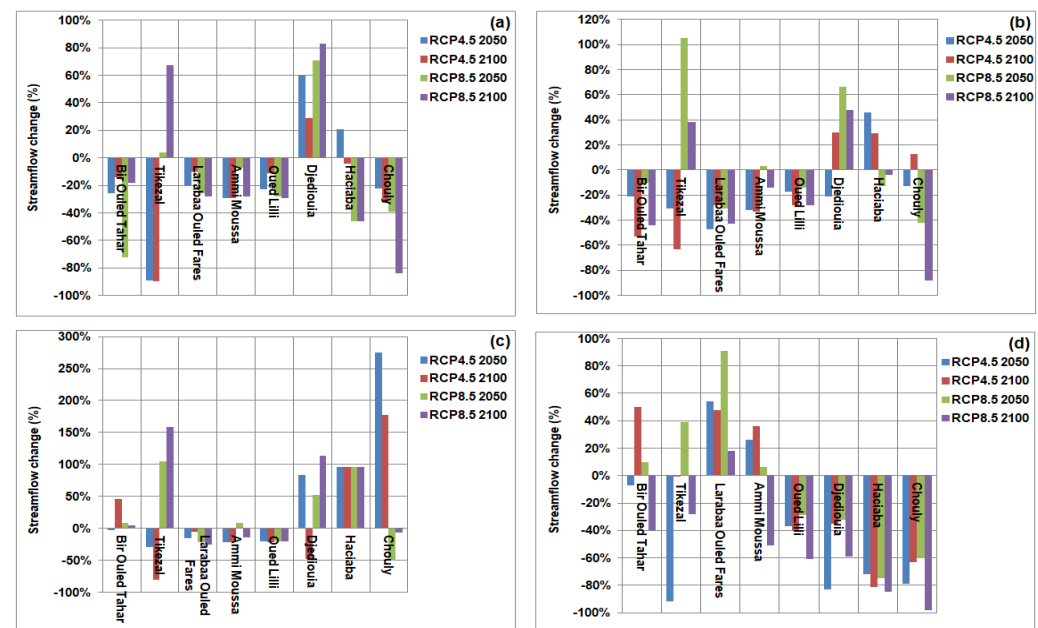
Figure 9. Changes in winter streamflow relative to the historical period under two scenarios (RCP4.5 and RCP8.5): (**a**) quantile mapping, (**b**) scaled distribution mapping, (**c**) quantile delta mapping, and (**d**) model RAW.
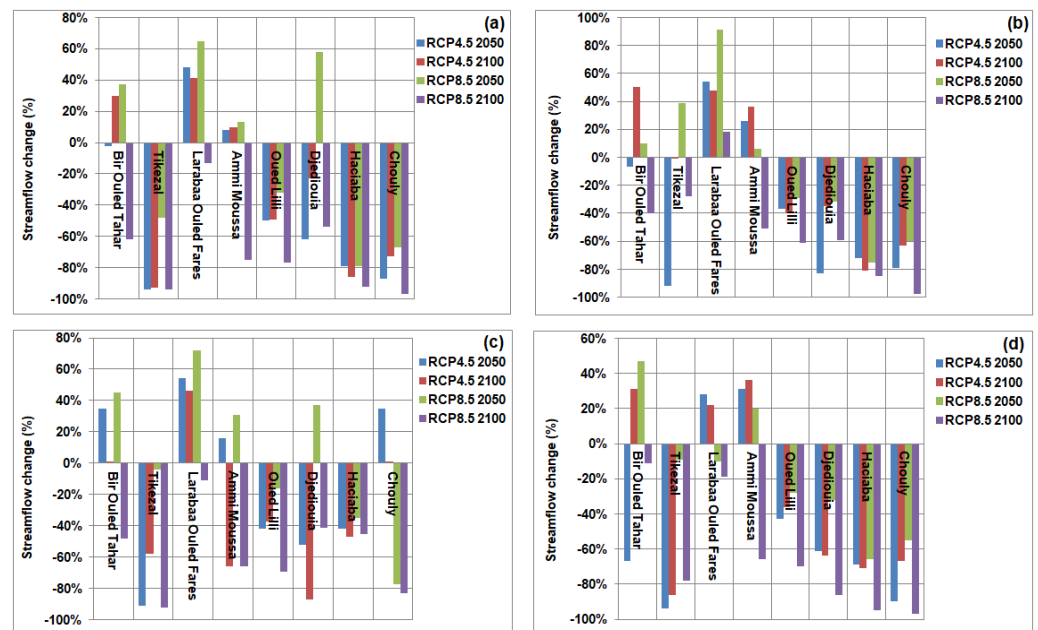
Figure 10. Changes in spring streamflow relative to the historical period under two scenarios (RCP4.5 and RCP8.5): (**a**) quantile mapping, (**b**) scaled distribution mapping, (**c**) quantile delta mapping, and (**d**) model RAW.
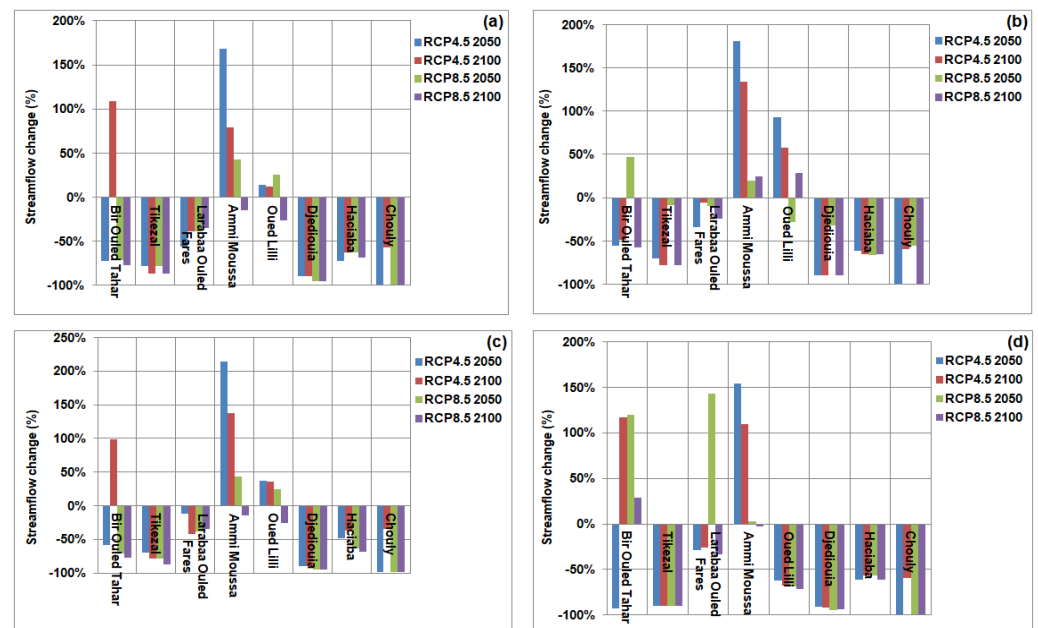
Figure 11. Changes in summer streamflow relative to the historical period under two scenarios (RCP4.5 and RCP8.5): (**a**) quantile mapping, (**b**) scaled distribution mapping, (**c**) quantile delta mapping, and (**d**) model RAW.

Under the RCP4.5 climate scenario, the rate of change of the predicted autumn flows ranges from −90% to +70% in the near term (2050s) and from −91% to +18% in the long term (2100s) when utilizing precipitation data corrected using the QDM approach (Table S6 and Figure 8). The rate of change under the RCP8.5 scenario, on the other hand, ranges from −1% to −89% and from −30% to −91% by 2100. Correction using the same algorithm (QDM) (Table S7 and Figure 9) revealed a rate change in winter ranging from −29% to +275% and from −80% to +177% by 2100 under the RCP4.5 scenario. With the RCP8.5 climate scenario, this rate of change is somewhat positive, ranging from −51% to

+105% and −25% to +158% by 2100. For the two climate scenarios, the rate of variation of future spring streamflow (Table S8 and Figure 10) varies from −92% to +72%. Using the QDM-algorithm-corrected models, an increase in summer flows (Table S9 and Figure 11) was found at two stations (Ammi Moussa and Oued Lilli station). This rise varies between +17% and +214% for the two periods (2050 and 2100) and the two scenarios. Summer flow is expected to decrease at the other stations (varying between −99 to −1%).

Finally, using raw precipitation data (Table S6 and Figure 8), the rate of change of expected autumn flows ranges between −91 and +33% in the near term (2050s) and −97 and +4% in the long term (2100s) under the RCP4.5 climate scenario. The change rate in the RCP8.5 scenario, on the other hand, fluctuates from −96% to −19% and from −97% to −30% over the 2100 horizon. Using raw data (Table S7 and Figure 9), the change rate in winters under the RCP4.5 scenario varies from −86 to +58% and −90 to +63% by 2100. With the RCP8.5 climate scenario, this goes from −74% to +53% by 2050 and −85% to +37% by 2100; this rate of change is slightly positive. For the two climate scenarios, the rate of variation of future spring streamflow (Table S9 and Figure 10) ranges from −94% to +47%. Using the QDM-algorithm-corrected models, an increase in summer flows (Table S9 and Figure 11) was found at three stations. This increase varies between +3% and +143% for the two time periods (2050 and 2100) and the two scenarios. Summer flow is expected to decrease at the other locations (varying between −3 and −99 percent).

In comparison with the corrective methods, a decrease in future flows in autumn, winter, and spring is projected in all of the watersheds analyzed; however, the rates of decrease are not synchronous. The rate of decrease is greatest when utilizing model outputs corrected by the QM approach, then raw model data, model outputs adjusted by the SDM method, and finally, model outputs corrected by the QDM method. In the summer, the average rate for all stations indicates an increase in future flows, albeit this rise is greater when model outputs corrected by the QDM approach are used than when the SDM and QM methods are used. The raw model data yielded the lowest rate of increase, followed by that corrected by the QM approach.

5. Discussion

The Zygos model was used in this study to investigate the impact of climate change on the CMT watersheds' water resources. The calibration/validation of the Zygos components on the datasets observed for the CMT basins reference period (1975–2012) allowed us to predict future flow evolution. After calibrating and validating the model by adjusting the model parameters, precipitation, and evapotranspiration, time series data from the Rossby Center Regional Climate Model (RCA4) RCA4-MPI-ESM-LR were substituted into the model and the flows were estimated. Before predicting probable changes in the Cheliff-Mactaa-Tafna (CMT) basins' hydrology, we adjusted the bias of the simulated precipitation data from the regional climate model RCA4-MPI-ESM-LR using three algorithms: quantile mapping, scaled distribution mapping, and quantile delta mapping.

5.1. Change in Precipitation

The results of this study showed that all bias correction methods improved the raw regional climate model (RCM) data to some extent. Nonetheless, the quality of RCM-adjusted precipitation is heavily dependent on the correction algorithm chosen, both for current and future climate conditions. The quantile delta algorithm, for example, is a stable and robust method that generates future time series with dynamics comparable to current conditions because it is based on observations [43]. In the case of the average, the QDM approach is regarded as the best method of correction. According to our analysis, the amount of precipitation varies from one station to another. Under the two scenarios, they fluctuate between −14 and +35% for all stations. This variation is between −32 and +34% for the SDM method, −45 and 05% for the QM method, and −37 and 14% for raw data.

In comparison to the corrective methods (Figure 12), a drop in future precipitation in autumn, winter, and spring is projected in all of the watersheds analyzed. At the same time,

the rates of decrease are not synchronous among the correction methods. The rate of decline is greatest when utilizing model outputs corrected by the QM method, then raw model data, model outputs adjusted by the SDM method, and finally, model outputs corrected by the QDM method. In the summer, the average rate for all stations indicates an increase in future flows, albeit this rise is greater when model outputs corrected by the QDM approach are used than when the SDM and QM methods are used. The raw model data yielded the lowest rate of increase, followed by that corrected by the QM approach. Furthermore, we would like to point out that none of the correction methods used to account for the physical reasons of precipitation biases were used (e.g., temporal errors in the main circulation systems or errors in the settings of the clouds' processes and precipitation).
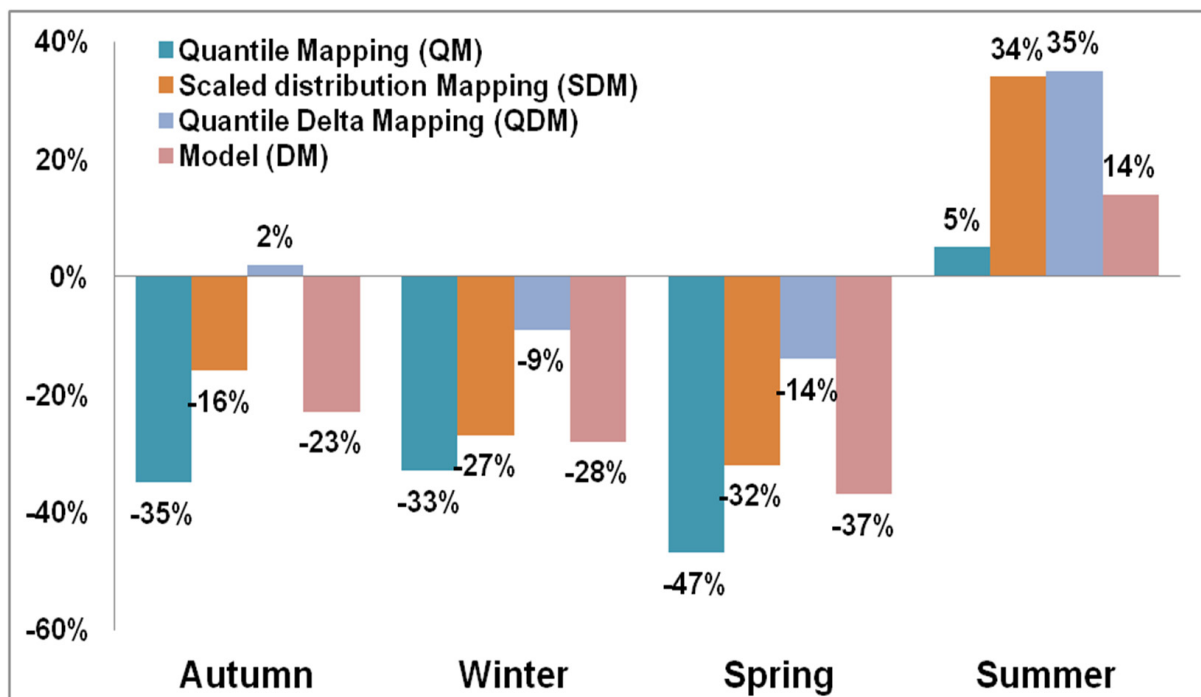
Figure 12. Seasonal precipitation mean variation over the CMT basins under the RCP4.5 and RCP8.5 climate scenarios.

5.2. Change in Streamflow

Figure 13 depicts the results of a comparison of the flows across two time periods, 2050 and 2100, using three correction methods: QM, SDM, and QDM, under two scenarios, RCP4.5 and RCP8.5. As indicated in Figure 13, all correction methods and all scenarios forecast a decrease in future seasonal flow, except for the rainy season (winter), which predicts an increase for the QDM correction method. The rate of decline is highest when utilizing model outputs corrected by the QM method, followed by model outputs corrected by the SDM method, raw model data, and finally, model outputs corrected by the QDM method.

Bias correction methods have a direct impact on the resulting hydrological simulations since they change the quality of the fit RCM data. Our findings show that it is possible to adjust climate model simulations in such a way that the features of the resulting mean for monthly flows are greatly reduced. Furthermore, by using higher-performing correction algorithms, variability ranges can be greatly lowered. Variability in the flow simulations, however, is caused not only by the various bias correction approaches, but also, to a significant degree, by the parameters that determine which winter flood peaks will be dominant and occur earlier due to excessive precipitation. Variations in the autumn flow simulations, on the other hand, are predicted to diminish dramatically, owing in part to the RCMs predicting less precipitation and more heat. Over the period from 1950 to 2016, the trend toward dryness between 0.8 and 0.9 °C since the 1980s in the coastal districts

of Algeria and since the 1990s on the high plateaus of Algeria was also observed [44]. Climate models predict that this warming will often exceed 1 °C on an annual scale, particularly in summer, between 1945 and 2100 under the RCP8.5 scenario [45]. The findings concerning precipitation decreases, seasonal, and yearly flows reflect previous findings in the literature for Algerian basins. According to the RCP 4.5 scenario, the prediction of the future evolution of rainfall in western Algeria shows a decline from −12% to −38% by the end of the 21st Century [46]. According to the two future scenarios, [47] discovered that drought episodes in the northwest areas are anticipated to be more severe and of longer lengths than in the past, particularly during the hot season (between May and September) between 2021 and 2071. Taïbi et al [48] discovered that the availability of surface water collected at the Ain Dalia dam in northeastern Algeria is likely to decline by 5% to 13% by 2050 and by 21% to 44% by 2100. Hadour et al [49] found similar results in some basins in the northwestern Algeria region, and Zeroual et al [50] found similar results in the Algerian-Hodna-Soummam basins.
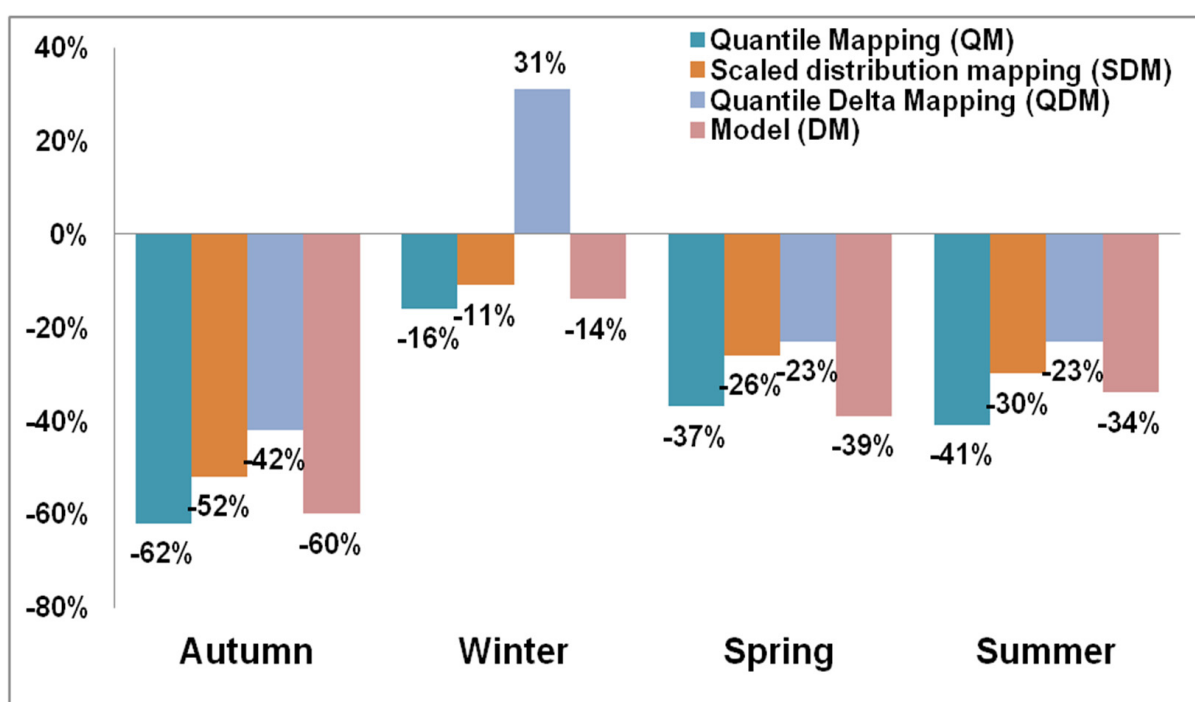
Figure 13. Seasonal streamflow mean variation over the CMT basins under the RCP4.5 and RCP8.5 climate scenarios.

6. Conclusions

The impact of climate change on the hydrology of the Cheliff-Mactaa-Tafna (CMT) basins was investigated using a CORDEX-Africa adjusted bias set on two climate projection scenarios, RCP 4.5 and RCP 8.5, of the concentration pathway representative of precipitation and temperature. Zygos simulates streamflow and the distribution mapping bias correction methods of quantile mapping (QM), quantile delta mapping (QDM), and scaled distribution mapping (SDM) to improve precipitation, temperature, and streamflow simulations utilizing a lumped approach. The bias correction algorithm chosen is critical in assessing the effects of climate change. The performance of the three bias correction algorithms (QM, QDM, and SDM) modulating the climate change signal of precipitation over six mountainous watersheds in northeastern Algeria was compared in this study. The capability of these corrective methods was assessed by modeling flows using the Zygos conceptual hydrological model. This led to various conclusions. Improvement was obtained for future data using all bias correction approaches, with varying rates of change. The RCM's raw outputs are highly skewed, making them unsuitable for direct use in analyzing

the consequences of climate change. The RCM simulations portrayal is largely dependent on region and season. Although bias correction methods have the potential to improve the performance of precipitation and temperature reproduction, their final findings are heavily influenced by the bias correction approaches. In our study area, all correction methods and both scenarios predicted a decrease in future seasonal flow, except for the rainy season (winter), which predicts an increase for the QDM method. The rate of decline is greater when utilizing model outputs corrected by the QM method, followed by model outputs corrected by the SDM method, raw model data, and finally, the QDM method. Future climate-corrected precipitation projections revealed significant variations over time. Most years will see high rainfall; however, certain years will experience low average precipitation when compared to the observed data.

Predicted rainfall and flow will also influence crop choices, cropping patterns, crop rotations, crop management frameworks, planting times, cropping area extent, agricultural yields, and so on. Changes in land use and cover, changes in groundwater, river, and surface water levels, flooding, and soil erosion will be highly posed in urban areas. Furthermore, the study area is well known for its heritage and tourism. Thus, the study supplies environmentalists, urban planners, and water resource managers with clear information on future rainfall and flows. Rainwater harvesting, aquifer recharge, reforestation, and channeling excess water to the river through proper channels are all viable options for dealing with future excess rainfall.

References

1. Change, Intergovernmental Panel On Climate. *Climate Change*; IPCC: Geneva, Switzerland, 2014.
2. Mukheibir, P. Water access, water scarcity, and climate change. *Environ. Manag.* **2010**, *45*, 1027–1039.
3. Schewe, J.; Heinke, J.; Gerten, D.; Haddeland, I.; Arnell, N.W.; Clark, D.B.; Dankers, R.; Eisner, S.; Fekete, B.M.; Colón-González, F.J.; et al. Multimodel assessment of water scarcity under climate change. *Proc. Natl. Acad. Sci. USA* **2014**, *111*, 3245–3250.
4. Arnell, N.W.; Gosling, S.N. The impacts of climate change on river flow regimes at the global scale. *J. Hydrol.* **2013**, *486*, 351–364.
5. Hattermann, F.F.; Krysanova, V.; Gosling, S.N.; Dankers, R.; Daggupati, P.; Donnelly, C.; Flörke, M.; Huang, S.; Motovilov, Y.; Buda, S.; et al. Cross-scale intercomparison of climate change impacts simulated by regional and global hydrological models in eleven large river basins. *Clim. Chang.* **2017**, *141*, 561–576.
6. Theodossiou, N. Assessing the Impacts of Climate Change on the Sustainability of Groundwater Aquifers. Application in Moudania Aquifer in N. Greece. *Environ. Process.* **2016**, *3*, 1045–1061.
7. Hamed, Y.; Hadji, R.; Redhaounia, B.; Zighmi, K.; Bâali, F.; El Gayar, A. Climate impact on surface and groundwater in North Africa: A global synthesis of findings and recommendations. *Euro-Mediterr. J. Environ. Integr.* **2018**, *3*, 25.
8. Mokadem, N.; Redhaounia, B.; Besser, H.; Ayadi, Y.; Khelifi, F.; Hamad, A.; Hamed, Y.; Bouri, S. Impact of climate change on groundwater and the extinction of ancient "Foggara" and springs systems in arid lands in North Africa: A case study in Gafsa basin (Central of Tunisia). *Euro-Mediterr. J. Environ. Integr.* **2018**, *3*, 28.
9. Meehl, G.A.; Covey, C.; Delworth, T.; Latif, M.; McAvaney, B.; Mitchell, J.F.B.; Stouffer, R.J.; Taylor, K.E. The WCRP CMIP3 Multimodel Dataset: A New Era in Climate Change Research. *Bull. Am. Meteorol. Soc.* **2007**, *88*, 1383–1394.
10. Mearns, L.O.; Arritt, R.; Biner, S.; Bukovsky, M.S.; McGinnis, S.; Sain, S.; Caya, D.; Correia, J.; Flory, D.; Gutowski, W.; et al. The North American regional climate change assessment program: Overview of phase I results. *Bull. Am. Meteorol. Soc.* **2012**, *93*, 1337–1362.
11. Sillmann, J.; Kharin, V.V.; Zwiers, F.W.; Zhang, X.; Bronaugh, D. Climate extremes indices in the CMIP5 multimodel ensemble: Part 2. Future climate projections. *J. Geophys. Res. Atmos.* **2013**, *118*, 2473–2493. [CrossRef]
12. Teutschbein, C.; Seibert, J. Bias correction of regional climate model simulations for hydrological climate-change impact studies: Review and evaluation of different methods. *J. Hydrol.* **2012**, *456*, 12–29.
13. Themeßl, M.J.; Gobiet, A.; Heinrich, G. Empirical-statistical downscaling and error correction of regional climate models and its impact on the climate change signal. *Clim. Chang.* **2012**, *112*, 449–468.
14. Räisänen, J.; Räty, O. Projections of daily mean temperature variability in the future: Cross-validation tests with ENSEMBLES regional climate simulations. *Clim. Dyn.* **2013**, *41*, 1553–1568.
15. Teutschbein, C.; Seibert, J. Is bias correction of regional climate model [RCM] simulations possible for non-stationary conditions? *Hydrol. Earth Syst. Sci.* **2013**, *17*, 5061–5077.
16. Fang, G.H.; Yang, J.; Chen, Y.N.; Zammit, C. Comparing bias correction methods in downscaling meteorological variables for a hydrologic impact study in an arid area in China. *Hydrol. Earth Syst. Sci.* **2015**, *19*, 2547–2559.
17. Ahmed, K.F.; Wang, G.; Silander, J.; Wilson, A.M.; Allen, J.M.; Horton, R.; Anyah, R. Statistical downscaling and bias correction of climate model outputs for climate change impact assessment in the U.S. northeast. *Glob. Planet. Chang.* **2013**, *100*, 320–332.
18. Switanek, M.B.; Troch, P.A.; Castro, C.L.; Leuprecht, A.; Chang, H.-I.; Mukherjee, R.; Demaria, E.M.C. Scaled distribution mapping: A bias correction method that preserves raw climate model projected changes. *Hydrol. Earth Syst. Sci.* **2017**, *21*, 2649–2666.
19. Grenier, P. Two Types of Physical Inconsistency to Avoid with Univariate Quantile Mapping: A Case Study over North America Concerning Relative Humidity and Its Parent Variables. *J. Appl. Meteorol. Clim.* **2018**, *57*, 347–364.
20. Willems, P.; Vrac, M. Statistical precipitation downscaling for small-scale hydrological impact investigations of climate change. *J. Hydrol.* **2011**, *402*, 193–205.
21. Gudmundsson, L.; Bremnes, J.B.; Haugen, J.E.; Engen-Skaugen, T. Downscaling RCM precipitation to the station scale using statistical transformations–a comparison of methods. *Hydrol. Earth Syst. Sci.* **2012**, *16*, 3383–3390.
22. Hempel, S.; Frieler, K.; Warszawski, L.; Schewe, J.; Piontek, F. A trend-preserving bias correction–the ISI-MIP approach. *Earth Syst. Dyn.* **2013**, *4*, 219–236.
23. Bürger, G.; Murdock, T.Q.; Werner, A.T.; Sobie, S.R.; Cannon, A.J. Downscaling Extremes—An Intercomparison of Multiple Statistical Methods for Present Climate. *J. Clim.* **2012**, *25*, 4366–4388.
24. Cannon, A.J.; Sobie, S.R.; Murdock, T.Q. Bias correction of GCM precipitation by quantile mapping: How well do methods preserve changes in quantiles and extremes? *J. Clim.* **2015**, *28*, 6938–6959.
25. Casanueva, A.; Herrera, S.; Iturbide, M.; Lange, S.; Jury, M.; Dosio, A.; Maraun, D.; Gutiérrez, J.M. Testing bias adjustment methods for regional climate change applications under observational uncertainty and resolution mismatch. *Atmos. Sci. Lett.* **2020**, *21*, e978.

26. Mpelasoka, F.S.; Chiew, F.H.S. Influence of Rainfall Scenario Construction Methods on Runoff Projections. *J. Hydrometeorol.* **2009**, *10*, 1168–1183.
27. Van Roosmalen, L.; Sonnenborg, T.O.; Jensen, K.H.; Christensen, J.H. Comparison of Hydrological Simulations of Climate Change Using Perturbation of Observations and Distribution-Based Scaling. *Vadose Zone J.* **2011**, *10*, 136–150.
28. Muerth, M.J.; Gauvin St-Denis, B.; Ricard, S.; Velázquez, J.A.; Schmid, J.; Minville, M.; Caya, D.; Chaumont, D.; Ludwig, R.; Turcotte, R. On the need for bias correction in regional climate scenarios to assess climate change impacts on river runoff. *Hydrol. Earth Syst. Sci.* **2013**, *17*, 1189–1204.
29. Teng, J.; Potter, N.J.; Chiew, F.H.S.; Zhang, L.; Wang, B.; Vaze, J.; Evans, J.P. How does bias correction of regional climate model precipitation affect modelled runoff? *Hydrol. Earth Syst. Sci.* **2015**, *19*, 711–728.
30. Nguyen, H.; Mehrotra, R.; Sharma, A. Assessment of Climate Change Impacts on Reservoir Storage Reliability, Resilience, and Vulnerability Using a Multivariate Frequency Bias Correction Approach. *Water Resour. Res.* **2020**, *56*, e2019WR026022.
31. Achour, K.; Meddi, M.; Zeroual, A.; Bouabdelli, S.; Maccioni, P.; Moramarco, T. Spatio-temporal analysis and forecasting of drought in the plains of northwestern Algeria using the standardized precipitation index. *J. Earth Syst. Sci.* **2020**, *129*, 42.
32. Zerouali, B.; Mesbah, M.; Chettih, M.; Djemai, M. Contribution of cross time-frequency analysis in assessment of possible relationships between large-scale climatic fluctuations and rainfall of northern central Algeria. *Arab. J. Geosci.* **2018**, *11*, 392.
33. Bouabdelli, S.; Meddi, M.; Zeroual, A.; Alkama, R. Hydrological drought risk recurrence under climate change in the karst area of Northwestern Algeria. *J. Water Clim. Chang.* **2020**, *11*, 164–188.
34. Zeroual, A.; Assani, A.A.; Meddi, M.; Alkama, R. Assessment of climate change in Algeria from 1951 to 2098 using the Köppen–Geiger climate classification scheme. *Clim. Dyn.* **2019**, *52*, 227–243.
35. Benzater, B.; Elouissi, A.; Benaricha, B.; Habi, M. Spatio-temporal trends in daily maximum rainfall in northwestern Algeria (Macta watershed case, Algeria). *Arab. J. Geosci.* **2019**, *12*, 370.
36. Bouchelkia, H.; Belarbi, F.; Rémini, B. Estimated flows of suspended solids by the statistical analysis of outfall drainage basin of Tafna (Algeria). *Soil Water Res.* **2013**, *8*, 63–70.
37. Jones, C.; Giorgi, F.; Asrar, G. The Coordinated Regional Downscaling Experiment: CORDEX–an international downscaling link to CMIP5. *CLIVAR Exch.* **2011**, *16*, 34–40.
38. Kozanis, S.; Christoforides, A.; Efstratiadis, A. Scientific Documentation of Hydrognomon software [version 4]. Development of Database and Software Application in a Web Platform for the "National Database and Meterological Information". ITIA Research Team, National Technical University of Athens. Available online: https://www.itia.ntua.gr/en/docinfo/928/1/Documents/HydrognomonV4TheoryGR-V1,2 (accessed on 6 July 2022).
39. Charizopoulos, N.; Psilovikos, A. Hydrologic processes simulation using the conceptual model Zygos: The example of Xynias drained Lake catchment (central Greece). *Environ. Earth Sci.* **2016**, *75*, 777. [CrossRef]
40. Charizopoulos, N.; Psilovikos, A.; Zagana, E. A lumped conceptual approach for modeling hydrological processes: The case of Scopia catchment area, Central Greece. *Environ. Earth Sci.* **2017**, *76*, 632. [CrossRef]
41. Madsen, H. Automatic calibration of a conceptual rainfall–runoff model using multiple objectives. *J. Hydrol.* **2000**, *235*, 276–288.
42. Khazaei, M.R.; Zahabiyoun, B.; Saghafian, B.; Ahmadi, S. Development of an Automatic Calibration Tool Using Genetic Algorithm for the ARNO Conceptual Rainfall-Runoff Model. *Arab. J. Sci. Eng.* **2013**, *39*, 2535–2549.
43. Anandhi, A.; Frei, A.; Pierson, D.C.; Schneiderman, E.M.; Zion, M.S.; Lounsbury, D.; Matonse, A.H. Examination of change factor methodologies for climate change impact assessment. *Water Resour. Res.* **2011**, *47*. [CrossRef]
44. Taïbi, S.; Zeroual, A.; Meddi, M. Effect of autocorrelation on temporal trends in air-temperature in Northern Algeria and links with teleconnections patterns. *Theor. Appl. Climatol.* **2022**, *147*, 959–984. [CrossRef]
45. Zeroual, A.; Assani, A.A.; Meddi, H.; Bouabdelli, S.; Zeroual, S.; Alkama, R. Assessment of Projected Precipitations and Temperatures Change Signals over Algeria Based on Regional Climate Model: RCA4 Simulations. In *Water Resources in Algeria—Part I. The Handbook of Environmental Chemistry*; Negm, A.M., Bouderbala, A., Chenchouni, H., Barceló, D., Eds.; Springer: Cham, Switzerland, 2020; Volume 97, pp. 135–159. [CrossRef]
46. Taïbi, S.; Anza, F.Z.H.; Zeroual, S. Etude de l'impact des changements climatiques sur la disponibilité des ressources en eau basée sur les simulations du modèle climatique régional RCA4: Cas du bassin de Ain DALIA (Algérie). *Alger. J. Environ. Sci. Technol.* **2021**, *7*, 1860–1869.
47. Bouabdelli, S.; Zeroual, A.; Meddi, M.; Assani, A. Impact of temperature on agricultural drought occurrence under the effects of climate change. *Theor. Appl. Climatol.* **2022**, *148*, 191–209.
48. Taïbi, S.; Zeroual, A.; Melhani, N. Evaluation de deux méthodes de correction de biais des sorties de modèles climatiques régionaux Cordex-Africa pour la prévision des pluies: Cas du bassin côtier oranais. *Proc. Int. Assoc. Hydrol. Sci.* **2021**, *384*, 213–218. [CrossRef]
49. Hadour, A.; Mahé, G.; Meddi, M. Watershed based hydrological evolution under climate change effect: An example from North Western Algeria. *J. Hydrol. Reg. Stud.* **2020**, *28*, 100671.
50. Zeroual, A.; Meddi, M.; Bensaad, S. The impact of climate change on river flow in arid and semi-arid rivers in Algeria. *IAHS-AISH Proc. Rep.* **2013**, *359*, 1–6.
51. Piani, C.; Haerter, J.O.; Coppola, E. Statistical bias correction for daily precipitation in regional climate models over Europe. *Theor. Appl. Climatol.* **2010**, *99*, 187–192.

52. Ringard, J.; Seyler, F.; Linguet, L. A Quantile Mapping Bias Correction Method Based on Hydroclimatic Classification of the Guiana Shield. *Sensors* **2017**, *17*, 1413. [CrossRef]
53. Li, C.; Sinha, E.; Horton, D.E.; Diffenbaugh, N.S.; Michalak, A.M. Joint bias correction of temperature and precipitation in climate model simulations. *J. Geophys. Res. Atmos.* **2014**, *119*, 13–153.